

WIND ENERGY MAPPING USING SYNTHETIC APERTURE RADAR

C. B. Hasager

Risoe National Laboratory, Wind Energy and Atmospheric Physics Dept.,
P.O.Box 49, 4000 Roskilde, Denmark
Charlotte.hasager@risoe.dk

ABSTRACT

Wind energy *off-shore* is gaining much interest due to the high wind power potentials. The need is to map wind climatology and regional wind patterns in coastal regions. In the WEMSAR (Wind Energy Mapping using Synthetic Aperture Radar) project three European sites will be covered near Norway, Denmark and Italy. Data to be used are from the ERS-2 C-band scatterometer with a 50 km resolution, from ERS-2 Ku-band and Topex Poseidon Ku-Band altimeter with a 7 km resolution and from SAR. The SAR data will be block averaged into 400 m resolution from ERS-2 C_VV, Radarsat C_HH and Envisat ASAR C_VV and C_HH beginning year 2000. For SAR data, the algorithm CMOD IFRE2 (Institute Francaise de Recherche pour L'Exploitation de la Mer) is used based on 3433 collocated pairs of buoys of NOAA and ECMWF (European Centre for Medium Range Weather Forecasts) with the accuracy of $\sqrt{2}$ m/s for a single retrieval. In the validation part of the WEMSAR project for wind energy retrieval, the ESA SAR (SAR.PRI (precision image format)) will be used because of the need for absolute calibration. Validation data are from long-term off-shore and coastal meteorological masts at the sites. Some masts are dedicated to wind power measurements including the roughness of sea and wave height. Optimal validation is crucial as wind energy varies with the third power of the wind speed. Also, the 10 or 19.5 m wind speeds will have to be calculated into 50-100 m height, i.e. the hub height of modern 600-1500 kW wind turbines. This calculation includes stability correction of the wind profiles. Wind analysis at mesoscale (1 km grid) with the non-hydrostatic KAMM (Karlsruhe Atmospheric Mesoscale Model) and WASP (the Risoe Wind Atlas Analysis and Application Program) for micro-siting will be used. The aim is to link from meteorological mast data to spatial mapping of the wind energy potential based on satellite SAR data in coastal areas.

1. Introduction

There are global plans for reduction of the CO₂ emissions according to the Kyoto protocol (IGBP, 1998). At the same time, the demand for electrical power is increasing in most societies. Therefore renewable energy sources are of interest. Wind power is one of the renewable energy sources that may contribute significantly worldwide. Today roughly 7% of the Danish power consumption is supplied by wind power. Within the next 30 years it is planned by the Danish government, that renewable sources (mainly wind power) should supply 35% of the total Danish electricity consumption. To achieve this goal the utilities take great interest in siting of wind turbines.

In many parts of the world where wind turbines are being planned, environmental authorities and local interest groups hold the point of view that wind turbine should not be placed due to e.g. bird migration, dwellings, tourism and so on. Therefore the number of attractive sites is limited. This has caused an interest in *off-shore siting* as the wind potential is relatively high at sea. An example of the estimated wind power production on land and off-shore at the Vindeby site in Denmark is shown in Figure 1. It is clear that the wind power potential is very much larger off-shore than on land. At this site an off-shore wind turbine park (11 turbines) has produced energy since 1991 (Barthelmie et al., 1994).

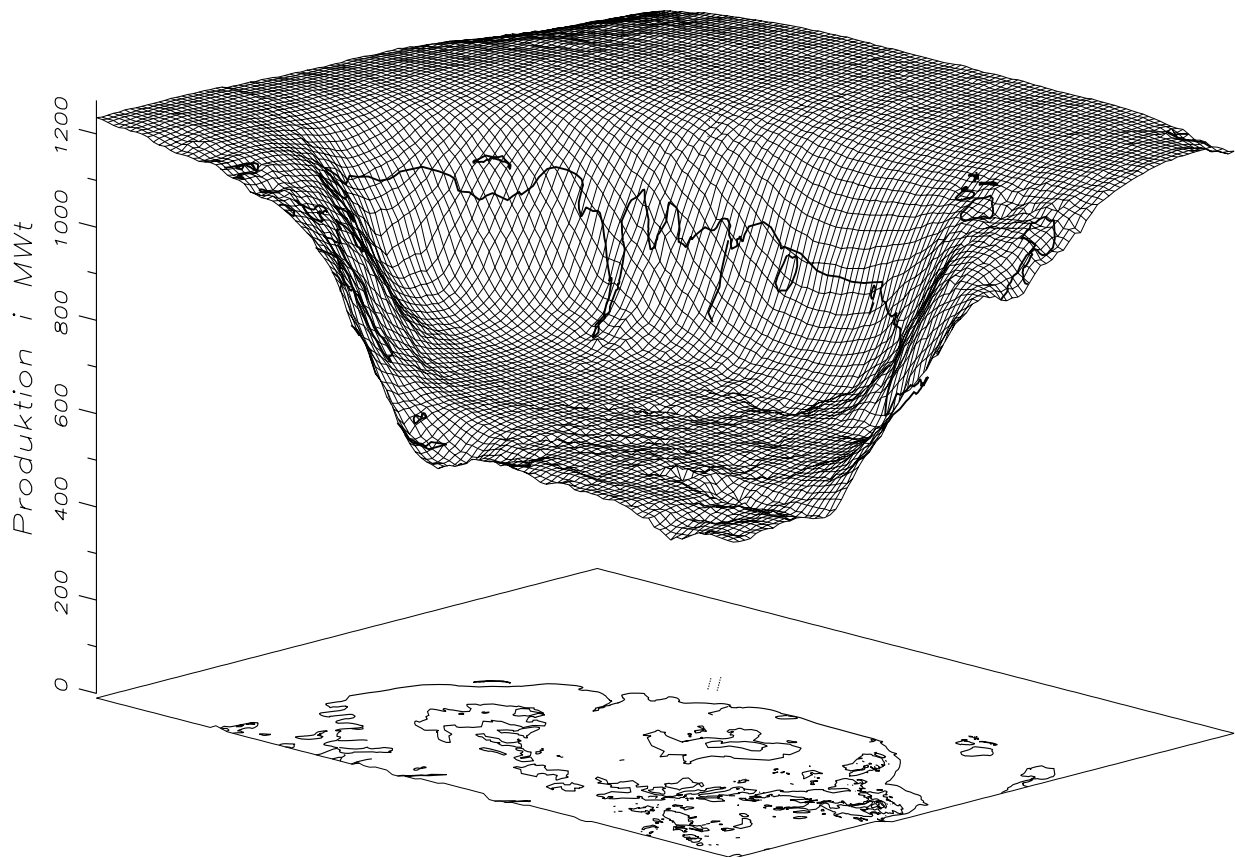


Figure 1. The estimated wind power production near Vindeby, Denmark. The Vindeby wind turbine farm is located 1 to 3 km off-shore (Courtesy of N.G. Mortensen).

Siting of wind turbines is usually performed by analysis of wind observations combined with information on orography, roughness and obstacles in the local terrain (Mortensen et al., 1993, Petersen et al., 1998). Wind statistics are obtained from long-term data series at one or few locations in the landscape and through modelling work calculated into maps for given areas, e.g. the European Wind Atlas (Troen and Petersen, 1989). An investigation on the mapping of wind energy resources off-shore by use of SAR satellite data will be undertaken within a new project. Spatial data of wind observations will provide a novel information source to current micrositing models.

2. Satellite radars

Satellite radars include scatterometers, altimeters and synthetic aperture radar (SAR) systems. Currently in operation are the ERS-2 C-band (5.3 GHz, VV) scatterometer, the Topex-Poseidon Ku-band altimeter, the ERS-2 Ku-band altimeter (13.8 GHz), the ERS-2 SAR C-band (VV) and the RADARSAT-1 SAR C-band (HH). For wind energy mapping also data from sensors that previously have been in operation may be of interest, here mainly the ERS-1 SAR scenes.

2.1 SAR

SAR data were collected first time from space with SEASAT in 1978. Since then other missions, among these the shuttle imaging radars (SIR), have delivered data (see Table 1) (from Hasager, 1997). However, only since ERS-1 was launched in 1991, has a continuous series of SAR data become available, currently provided by ERS-2 SAR and RADARSAT-1. In year 2000 the ASAR C-band (VV & HH) at ENVISAT will be launched and in year 2001 the RADARSAT-2 C-band (HH). Hence the future availability of SAR scenes is promising.

The radar antenna transmits microwaves with a controlled (known) strength, frequency and polarization. It is the backscattered signal of this electromagnetic radiation that is measured and projected onto a grid via a time- and space-dependent algorithm. For image processing it can be considered as a grid of pixels. The value in each pixel usually is the signal strength squared (with unit Volt² per pixel).

The mean reflection in a calibrated SAR image is called the backscatter coefficient, Φ_0 . It is dimensionless. It is proportional to the effect. Φ_0 is defined as a measure of the expected return signal from randomly distributed scattering elements in an area of 1 m² in the horizontal plane. Φ_0 is a function of surface parameters such as roughness, geometry and dielectric properties. Furthermore it is a function of radar observation parameters such as frequency, polarisation and incidence angle. SAR data are polarimetric. This means that the received and transmitted signal matrix can be described from coordinates horizontal (H) and vertical (V) to the incidence angle, relative to nadir for a plane surface. Φ_0 has a very large dynamic range, roughly $1 \cdot 10^5$, and therefore the values are recalculated with the logarithm (with base 10) into decibel (dB).

Table 1. SAR data available from satellites and shuttle missions. * means optically processed. All other scenes are digitally processed.

Name	Period	Band	Polarization	σ^0 (dB)
SEASAT	July-Sep. 1978	L	HH	22
SIR 1 (A)*	Nov. 1981	L	HH	50
SIR 2 (B)	Oct. 1984	L	HH	20-50
ALMAZ 1	1987-	S	HH	25-50
ALMAZ 2	May 91-Oct. 92	S	HH	25-50
ERS-1	July 1991-1996	C	VV	23
JERS-1	Feb. 1992-	L	HH	38.5
SIR 3(C)	Dec. 1993	L,C	HH VV HV VH	variable
		X	HH	variable
ERS-2	April 1995-	C	VV	23
RADARS AT	Nov. 1995-	C	HH	20-50

For technical reasons a chirp technique, i.e. a long pulse with modulations on the frequency, is emitted and after reception transformed into a short pulse value. The emitted pulses from the radar hit the objects in the resolution cell at the theoretically homogeneous scattering surface at different angles and times. Backscatter and surface penetration vary slightly according to the scattering media. The result is that the backscattered contribution from the various places within the resolution cell is changed to a different phase, power and polarization. Phase shift causes constructive or destructive interference to occur.

The SAR image constructed from a linear combination of all the individual scatters illuminated by the radar will vary around a mean value. When the amplitude is squared, the phase information is eliminated, but the brightness (intensity) differences are preserved. The standard deviation on brightness is dependent upon the number of looks. Number of looks refers to uncorrelated radar recordings of the same element under ideally the same conditions. To eliminate the unwanted scatter in Φ_0 , the radar system is constructed so that it "sees" the object several times and the signals (effect

values) are averaged. Hence the variance of the intensity is reduced. It is a non-coherent averaging performed in raw signal data by dividing the antenna into more "seeing segments" and thereby obtaining a larger number of uncorrelated recordings of the same resolution cell. As the number of effective looks is not determined by the user of SAR data, other tools have to be used to get rid of unwanted variance around the mean, the so-called speckle noise (FAO, 1993).

Speckle is a statistic fluctuation or uncertainty associated with the brightness in each pixel. Speckle noise is multiplicative. This means that the higher the mean reflection, the larger the spread. So in an area mapped with dark grey tones (low Φ_0), the speckle will generally be less than in brighter areas. Users can reduce speckle either by filtering techniques or by block-averaging. Filtering is performed in image data by averaging a number of pixels in a moving window and assigning the centre pixels new (estimated) values based on the local statistics appearing within the window (e.g. Hasager, 1997). Block-averaging is done by averaging a number of cells. Hence the spatial resolution is decreased. For ERS SAR the resolution cells are 25 m * 25 m, and it is foreseen that a 400 m * 400 m resolution will be adequate for estimation of off-shore wind resources. The swath of ERS SAR is 100 km.

SAR recording is independent of sunlight and the atmospheric damping of microwaves is very small at wavelengths larger than 3 cm (< 10 GHz). It means that the C-band energy (5.6 cm wavelength) is transmitted practically undisturbed through the atmosphere. Clouds and precipitation do not effect the recording.

2.2 Retrieval of wind speed and direction from SAR

Physical principle of using SAR to estimate the wind speed is through the correlation between capillary waves at the sea surface and the backscattered signals. Although the CMOD4 (Stoffelen & Anderson, 1993, see Offiler, 1994) and CMOD IFRE2 algorithms were developed originally for scatterometer data, the models have been shown to be useful for SAR data too (e.g. Offiler, 1994, Mastenbroek, 1998, Korsbakken & Furevik, 1998).

The empirical methodology of retrieving wind speeds from C-band VV scatterometer is well-established. The method is based on derivation of fitting functions between ocean wind speeds and radar parameters. There are two well-know methods, the CMOD4 (Stoffelen and Anderson, 1993) (implemented at ESA in 1993 for operational fast-delivery wind product) and the CMOD IFR2 (Quilfen et al., 1998) (an off-line product from IFREMER, i.e. Institute Francaise de Recherche pour L'Exploitation de la Mer). CMOD IFRE2 is based upon wind speed data from 3433 collocated pairs of NOAA buoys and ECMWF model results. The estimated model tranfer function (MTF) is derived from the relationship between wind speed at 10 m, Φ_0 , the incidence angle of the radar beam and the azimuth direction of the mean wind vector. The relationships are implemented in analytic form with the supplied coefficients used to generate look-up tables of as a function Φ_0 , incidence angle of the radar beam and the wind direction (Offiler, 1994).

The models are very sensitive to Φ_0 . Therefore SAR scenes in the precision image format, SAR.PRI, will be used because these can be further calibrated by the user (e.g. Scoon et al., 1996).

Wind direction can in some cases be estimated from wind streaks in the SAR scenes. If not, wind direction will have to be taken from NWP models or meteorological observations. Wind streaks were visible in approximately 65% of the scenes used in a study on winds in a coastal region in the Baltic Sea (Lehner et al., 1998, Horstmann et al. 1998). In this work the wind streak direction was determined by applying a two-dimensional Fourier transform (FFT) to a sub-set of the radar scene. It should be noted however, that the wind streaks will not be aligned with the mean wind vector but offset due to Ekman turning. For a Dutch waddensee study (Mastenbroek, 1998) this angular difference was found to be about 10°. In near-coastal regions (> 3 km from shore) the wind direction was shown to be measured from SAR wind streaks to an accuracy of 5°(Lehner et al., 1998). The angular deviation

between wind streaks and the mean wind vector will be dependent upon the height above surface, the static stability and internal boundary layer(s). This/these will be present for off-shore flow (i.e. flow from the land to the sea) as opposed to on-shore flow from the open sea (fetch-unlimited flow).

2.3 Roughness of the sea

It is well-known that the wind generates capillary waves at the sea surface and that Charnock's relation provides a formula to calculate the roughness (z_0 in m) from the friction velocity (u_* in m/s) and the acceleration of gravity (g in m s^{-2}). The equation reads $z_0 = 0.015 u_*^2 / g$ (Charnock, 1955 *in* Stull, 1991). Studies have shown that in fetch-limited seas the roughness is dependent upon fetch. In the Danish seas a constant of 0.018 seems more appropriate than the original value of 0.015. For open seas 0.011 is generally recommended (Johnson et al., 1998). It is important to include these roughness effects in microscale models (Astrup et al., 1999). A LINearized COMputational model (LINCOM) useful for flow over hilly terrain (Troen & de Baas, 1986), is combined with a microscale aggregation model useful for flow over terrain with variations in surface roughness (Hasager & Jensen, 1999) and a model for the sea surface roughness (Astrup et al., 1999, Petersen et al. 1998). The parametrization yields relatively larger roughness near the shore and at larger distances approach the Charnock relationship. The roughness step change between the land and sea is a significant parameter.

Recently meteorological data sampled from sea-masts at the Vindeby site has been analysed in relation to fetch and stability, and it was demonstrated that the effect of stability is significant (Petersen et al. 1998, Lange and Højstrup, *subm.*). This supports the results of (Frank et al, *subm*) that demonstrates that a correct description of stratification is more important than applying a fetch dependent sea roughness.

Drawbacks of NWP and planetary boundary layer models (PBL) are that they are too coarse compared to SAR satellite data (Offiler, 1994). NWP/PBL results have been used extensively for comparison to e.g. scatterometer wind products. For SAR algorithms it becomes important to combine high-resolution mesoscale models e.g. KAMM with a 1 km resolution (Karlsruhe Atmospheric Mesoscale Model) and WasP micro-siting model as well as long-term meteorological observations at sea-masts. Further, to ascertain the static stability, sea and land surface temperatures (SST/LST) should be derived from NOAA AVHRR and ATSR and combined with air temperature observations to the ocean wind speed observations. These methods will be used in a project in years 2000-2002. The project WEMSAR, Wind Energy Mapping Using Synthetic Aperture Radar, is a EU funded project with partners from the Nansen Environmental and Remote Sensing Center (Norway), NEG Micon and Risø (Denmark) and ENEA (Italy).

Studies on the state of the sea surface will be very important for improving the SAR wind derivations. The physical link between wind speed and generation of capillary waves is dependent upon a long list of factors e.g. tidal currents, slicks, bathymetry, wave age, temperature, viscosity, fetch, atmospheric stratification, coastal orography, land-sea breezes and low-level jets over cold seas (Petersen et al., 1998). Some of these parameters have been investigated in part in relation to methods for wind retrieval from SAR e.g. in the VIERS model (Janssen et al., 1998) and in so-called SWA (SAR Wind Algorithm) method originally developed by (Vachon et al. 1994, *see* Korsbakken et al., 1998).

2.4 Briefly on scatterometer and altimeter

Scatterometer data has a resolution of 50 km x 50 km and covers a swath of 500 km. The working principle is that a short pulse is emitted towards the surface and the returned signal is recorded. The incidence angles of the side-looking instrument are between 18° and 59°. The wind direction is not retrieved directly, but derived through a first guess approach on wind direction based on NWP. The backscatter from the three independent backscatter measures (fore, mid and aft beams) normally yields a 180° ambiguity on wind direction solved through triplets within a mathematical model (Ebuchi &

Graber, 1998, Kramer, 1996). The specification of 2 m s^{-1} or 10% in rms and $\pm 20^\circ$ in wind direction is met for the $2\text{-}24 \text{ m s}^{-1}$ wind speed interval. In some cases (i.e. for a dataset where near-neutral stability is fulfilled) the accuracy is 1.5 m s^{-1} by the CMOD4 (Offiler, 1994).

The K-band altimeters on-board ERS and Topex-Poseidon have footprints varying from less than a km over calm seas to several km over rough sea. The resolution is 7 km. The altimeter transmits short pulses from nadir and receives the backscattered signals. From analysis of the form of the echo pulse and the timelag, it is feasible to estimate the height of the surface (ocean or land) and the significant wave height. Wind direction is not retrieved (Kramer, 1996).

ACKNOWLEDGEMENTS

Funding from EU in project ERK6-CT-1999-00017 is acknowledged.

REFERENCES

Astrup, P., Larsen, S.E., Rathmann, O. and Madsen, P.H., 1999: WASP engineering –Wind flow modelling over land and sea. *In* Wind Engineering into the 21st Century, Larsen, Larose & Livesey (eds.). Balkema, Rotterdam, pp 179-184

Barthelmie, R.J, Courtney, M.S., Højstrup, J. & Sanderhoff, P., 1994: The Vindeby Project: A description. Risø Report R-741 (EN). Risø National Laboratory, Roskilde, Denmark

Ebuchi, N. & Graber, H. C., 1998: Directivity of wind vectors derived from the ERS-1/AMI scatterometer, *J. Geophys. Research*, **103**, pp 7787-7798

FAO, 1993: Remote Sensing Centre. Radar imagery. Theory and interpretation. Lecture Notes, ESA FAO Rome, p 103

Frank, H.P, Larsen, S.E., & Højstrup, J. (subm): Simulated wind power off-shore using different parameterizations for the sea surface roughness. *Wind Energy*.

Hasager, C.B., 1997: Surface fluxes in heterogeneous landscape. (Ph.D. thesis). Risø-R-922(EN). Risø National Laboratory, Roskilde, Denmark. p180

Hasager, C.B. and Jensen, N.O., 1999: Surface-flux aggregation in heterogeneous terrain. *Q. J. R. Meteor. Soc.*, **125**, pp 2075-2102

Horstmann, J., Koch, W., Lehner, S. and Rosenthal, W., 1998: Ocean wind fields and their variability derived from SAR, *ESA-Earth Observation Quarterly*, **59**, pp 8-12

Janssen, P.A.E.M., Wallbrink, H. Calkoen, C.J., von Halsema, D., Oost, W.A. and Snoeij, P. :VIERS-1 scatterometer model. *J. Geophys. Research*, **103**, pp 7807-7832

IGBP, 1998: The terrestrial carbon cycle: Implications for the Kyoto Protocol, *Science*, **280**, pp 1393-1394

Johnson, H. K., Højstrup, J., Vested, H.J. & Larsen, S.E., 1998: On the dependence of sea surface roughness on wind waves. *J. Phys. Oceanogr.*, **28**, pp 1702-1716

Korsbakken, E. & Furevik, B., 1998: Wind field retrieval from SAR compared with scatterometer wind field during ERS Tandam phase. *ESA-Earth Observation Quarterly*, **59**, pp 23-26

Korsbakken, E., Johannessen, J.A. and Johannessen, O.M., 1998: Coastal wind field retrievals from ERS synthetic aperture radar images. *J. Geophys. Research*, **103**, C4, pp 7857-7874

Kramer, H.J., 1996: Observation of the Earth and Its Environment. Springer. 3rd enlarged ed., Berlin. p960

Lange, B. & Højstrup, J. (subm.): A validation study of WAsP for offshore applications. ICWE special issue of the J. of Wind Engineering and Industrial Aerodynamics (submitted)

Lehner, S., Horstmann, J., Koch, W. and Rosenthal, W., 1998: Mesoscale wind measurements using recalibrated ERS SAR images. *J. Geophys. Research*, **103**, pp 7847-7856

Mastenbroek, K., 1998: High-resolution wind fields from ERS SAR. *ESA-Earth Observation Quarterly*, **59**, pp 20-22

Mortensen, N.G., Landberg, L., Troen, I. and Petersen, E.L., 1993: Wind Atlas analysis and application Program (WAsP). Risø National Laboratory, Roskilde, Denmark

Offiler, D., 1994: The calibration of ERS-1 satellite scatterometer winds, *J. Atmospheric and Oceanic Technology*, **11**, pp1002-1017

Petersen, E.L., Mortensen, N.G., Landberg, L., Højstrup, H. & Frank, H., 1998: Wind power meteorology. Part II: Siting and models. *Wind Energy* **1**, pp 55-72

Quilfen, Y., Chapron, B., Elfouhaily, T., Katsaros, K. and Tournadre, J., 1998: Observation of tropical cyclones by high-resolution scatterometry. *J. Geophys. Research*, **103**, pp 7767-7786

Scoon, A, Robinson, I.S. and Meadows, P.J., 1996: Demonstration of an improved calibration scheme for ERS-1 SAR imagery using a scatterometer wind model. *Int. J. Remote Sensing*, **17**, 2, pp 413-418

Stoffelen, A. and Anderson, D.L.T., 1993: Wind retrieval and ERS-1 scatterometer radar backscatter measurements. *Advance Space Research*, **13**, pp53-60

Stull, R.B., 1991: An introduction to boundary layer meteorology. Kluwer Academic Publishers. p666

Troen, I. & de Baas, A., 1986: A spectral diagnostic model for wind flow simulation in complex terrain. *Proceedings of the European Wind Energy Association Conference & Exhibition*, Rome, pp 37-41

Troen, I. and Petersen, E.L., 1989: European Wind Atlas. Risø National Laboratory, Roskilde, Denmark, p656.